Underground Utilities Sensing with Augmented Reality

Tian Xia[1], Professor

Dryver Huston, Mauricio Pereira, Dan Orfeo, Dylan Burns, Robert Farrell, Keith Thomas, Justin Bond, Yan Zhang,

School of Engineering, University of Vermont, Burlington, VT

Supported by US National Science Foundation grants 1647095 and 1640687

Project Goals and Objectives

- Develop 3-d underground utilities map fusing ground penetrating radar, pipe robot telemetry, new construction observations and historical records.
- Place condition and operation sensors into at key locations.
- Use fiber optic high-speed telecommunications network – Burlington Telecom fiber optic network (Burlington and part of Winooski)
- Create Underground Infrastructure Information Model database for use in infrastructure management and planning.
- Integrate cybersecurity measures into design decisions.

Long-term Vision

- Living information system
- Model of underground infrastructure in 3D
- Sensors – leak, flow, temperature, chemical etc.
- High-speed data network to sensors and users
- Improved operations

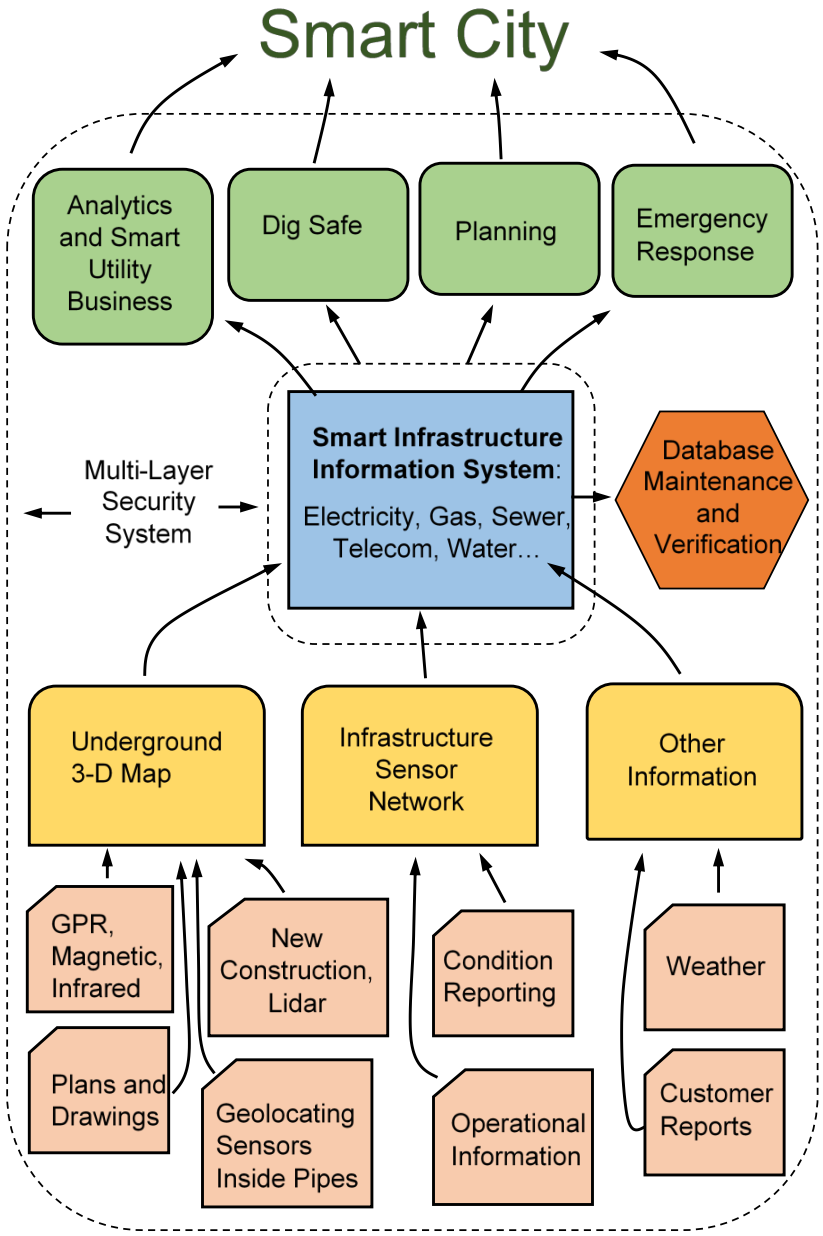

On-Going Research

- **Ground Penetrating Radar**
- **Magnetometer sensor with LoRa network**
- **Augmented Reality (AR) for positioning and mapping**
- **Virtual Reality (VR) to facilitate sensing operations**

Ground Penetrating Radar

- Big need for low-cost, standoff, subsurface inspection techniques – roadway and building condition assessment, buried utility location, through-wall sensing (firefighters, security), defense, archeology.

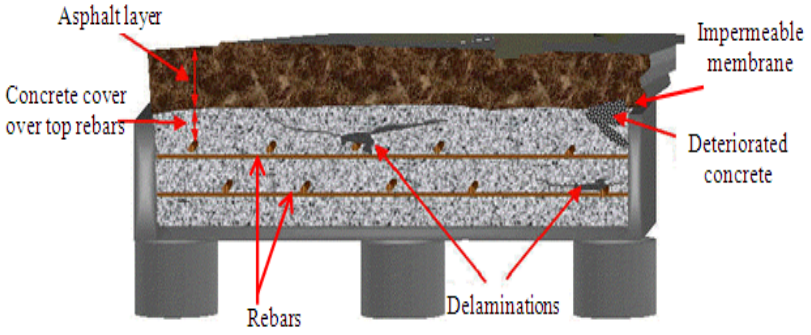

Current GPR Literature

Ground coupled GPR is dominant:

- Good penetrating capability and low sensitivity to interference.
- However, low survey speed,

  i.e. 1~2 mph, causes traffic disturbance.

Air-launched GPR:

- Low pulse repetition frequency

  ~ 50 incident pulses/s

- Low spatial resolution

  >0.3 m inspection gap @ 30 mph survey speed.

GPR Operating Principles

- Subsurface medias of different dielectric constants
- From the signal travel time and the amplitude of the reflected signal, a target feature inside a material can be identified and the depth of the target can be measured

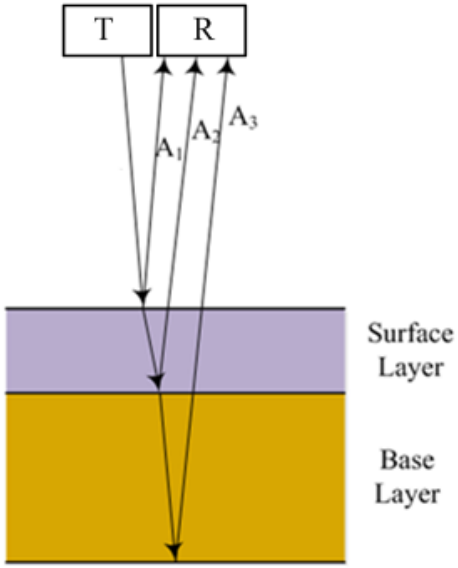

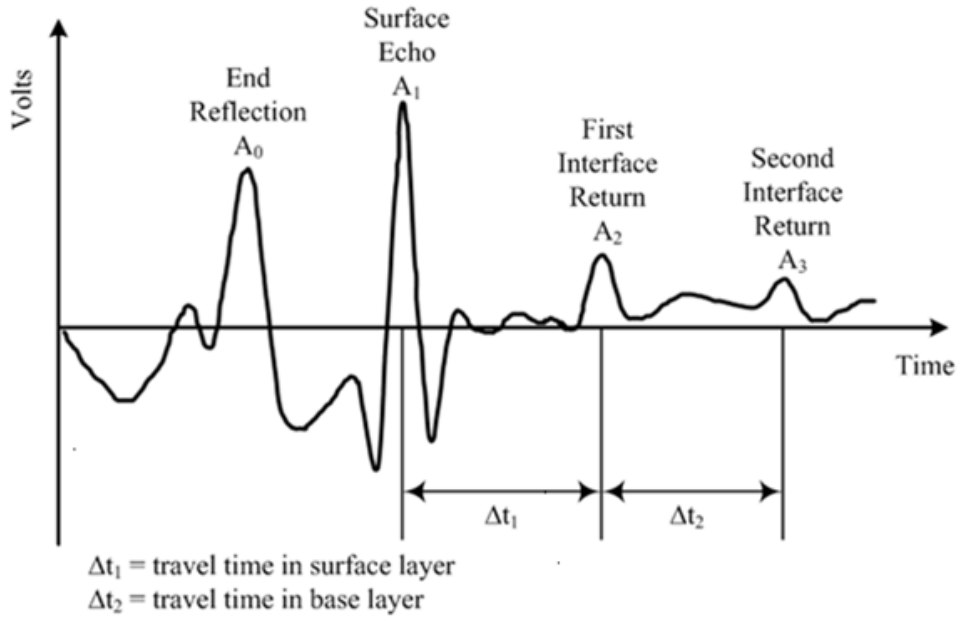

A-Scans, B-Scans and Hyperbolas

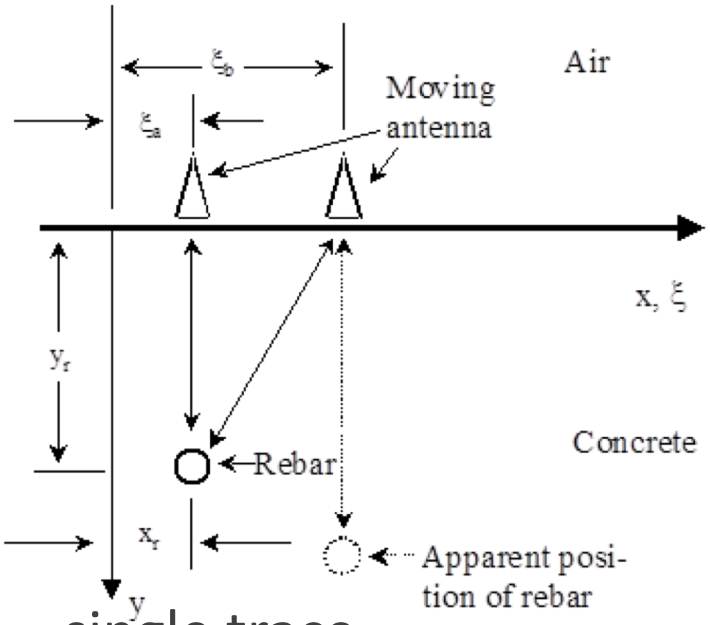

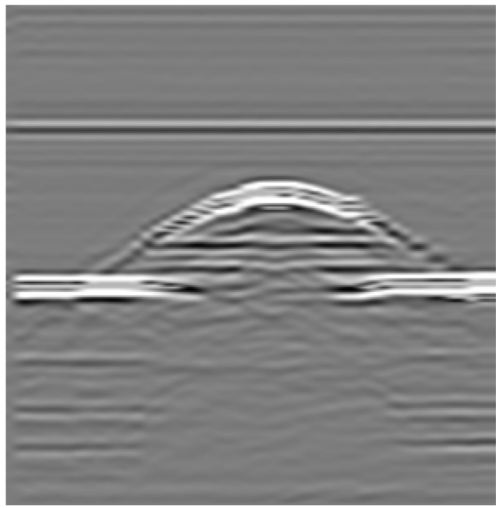

B-scan of aluminum cylinder

A-scan – single trace

B-scan – stack of traces assembled into 2-D image

Tomographic reconstruction

Hyperbolas result from moving antenna while collecting data

Innovative High-Speed Tomographic GPR

Targeted Features:

- Air-launched GPR;
- Enable driving speed survey;
- Fine high resolution: 1 cm;
- Wide area coverage – parallel lanes inspection;
- Good penetrating capability.
- Quickly scan and produce tomographic 3-D images of underground infrastructure.

The congested nature of urban underground infrastructure likely requires resolving problems related to multistatic and phased array GPR.

GPR Hardware Design

GPR system design and integration

- High fidelity UWB pulse generator
- FPGA based digital controller
- UWB high impedance matching antennas
- High speed data acquisition

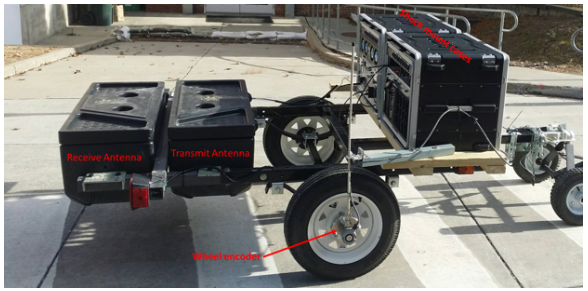

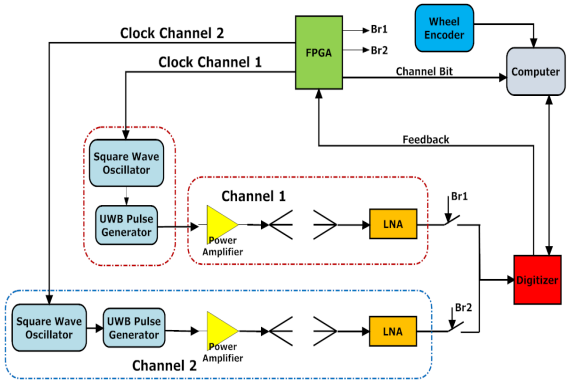

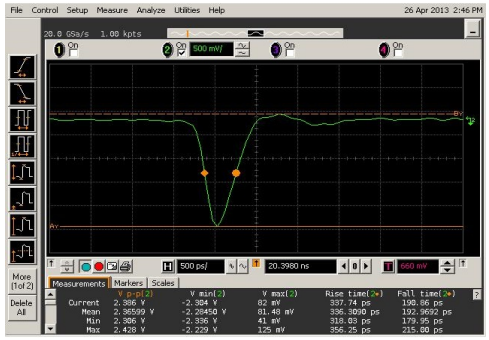

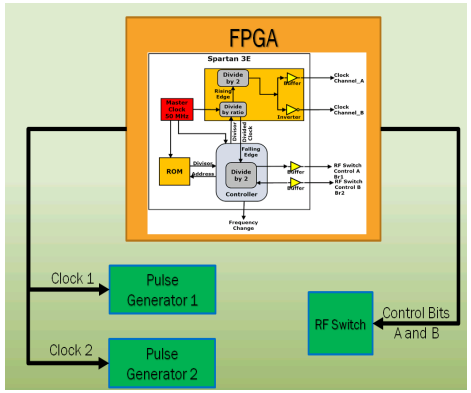

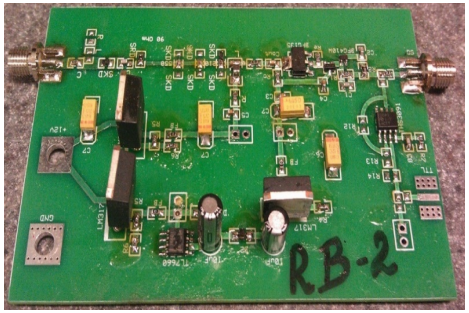

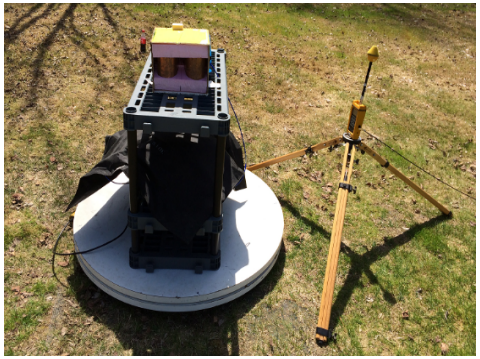

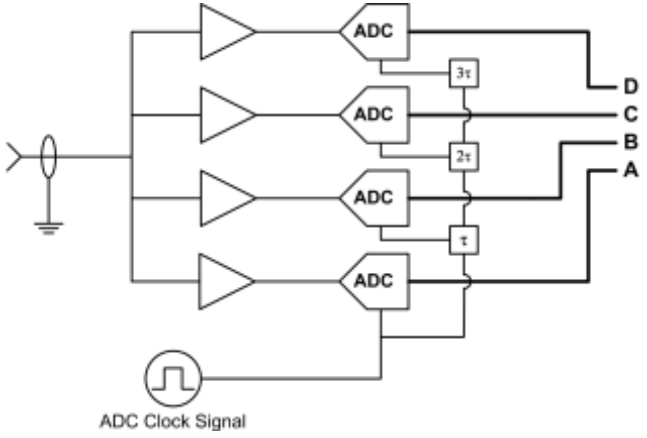

GPR Software

1. Data Organization
2. Graphic User Interface
3. Web-GIS Database
4. GPR Signal Processing

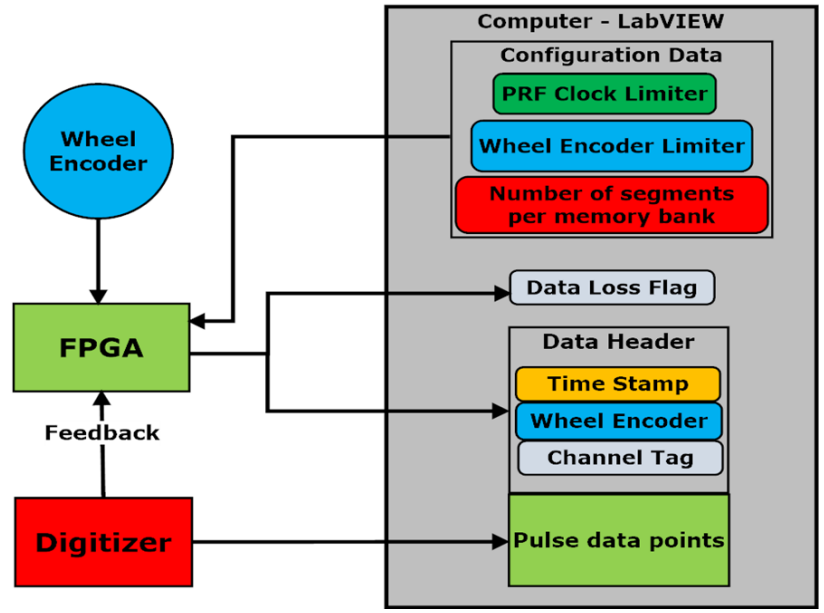

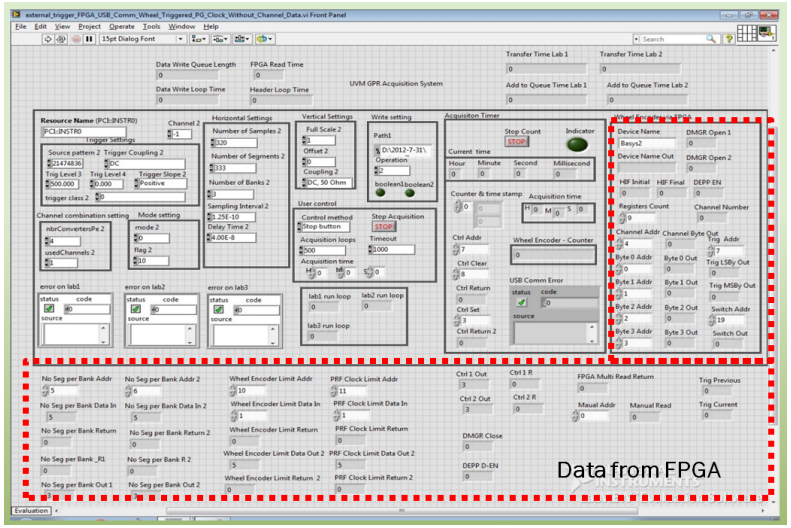

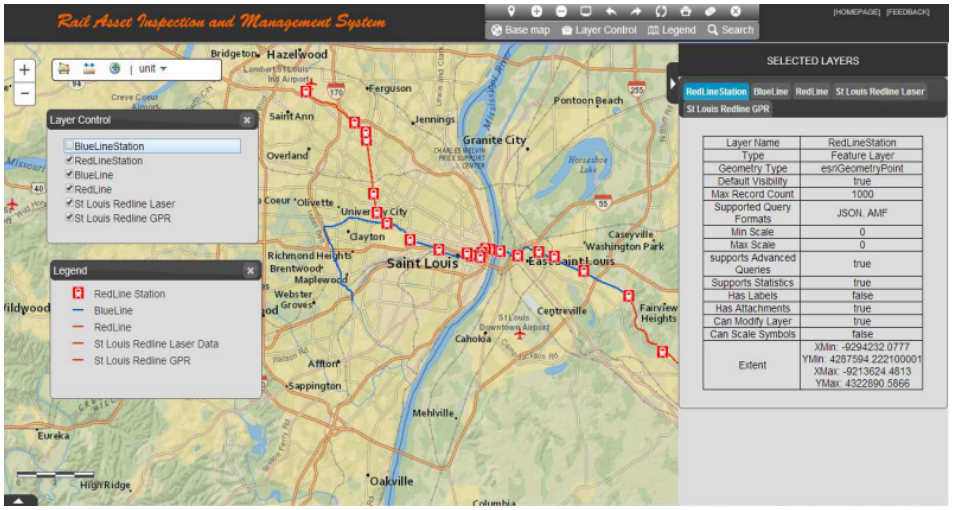

GPR Signal Processing

- Feature characterizations
  - Radar image enhancement: de-noising, clutter removal, vibration effect compensation, adaptive scaling…
  - Statistical signal processing: 2D entropy analysis
  - Feature interpretation: spectrum analysis, curve fitting, correlation, pattern recognition, etc.
- Positioning and mapping
- Burying media property characterizations

Algorithm 1: Singular Region Detection Using 2D Entropy Analysis

To effectively detect region of interest from the big data set

The survey data volume can easily surpass tens of GBs, while less than 1% data are critical.

Method: Renyi's Entropy + OTSU's data segment

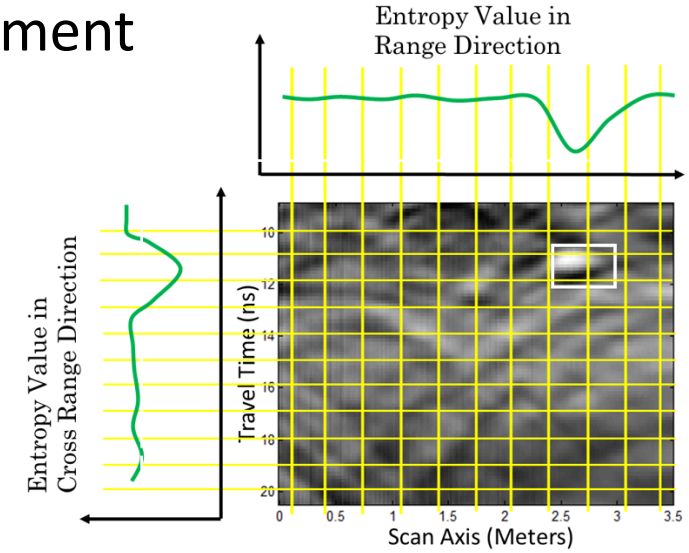

$$Y(t) = D(t) + S(t);$$

D(t): the reflection signal from the object;
S(t): systematic interference signal

Normalization: $y_i(t) = \frac{\|Y_i(t)\|^2}{\sum_{i=1}^{M}\|Y_i(t)\|^2}$

Renyi's Entropy:

$$E_\alpha(t) = \frac{1}{1-\alpha}\log_e\langle\sum_{i=1}^{M}[y_i(t)]^\alpha\rangle$$

OTSU's thresholding: evaluating image region's homogeneity through intensity variance assessment.

$$\sigma_B^2(k_1^*, k_2^*) = \max_{k_1,k_2\epsilon[A_{\min},A_{\max}]}\sigma_B^2(k_1, k_2).$$

Railroad Inspection

The system was tested at MBTA Boston and Metro St. Louis. Over 100 GB data collection.

UVM GPR system mounted on the railroad vehicle

The team at the test field

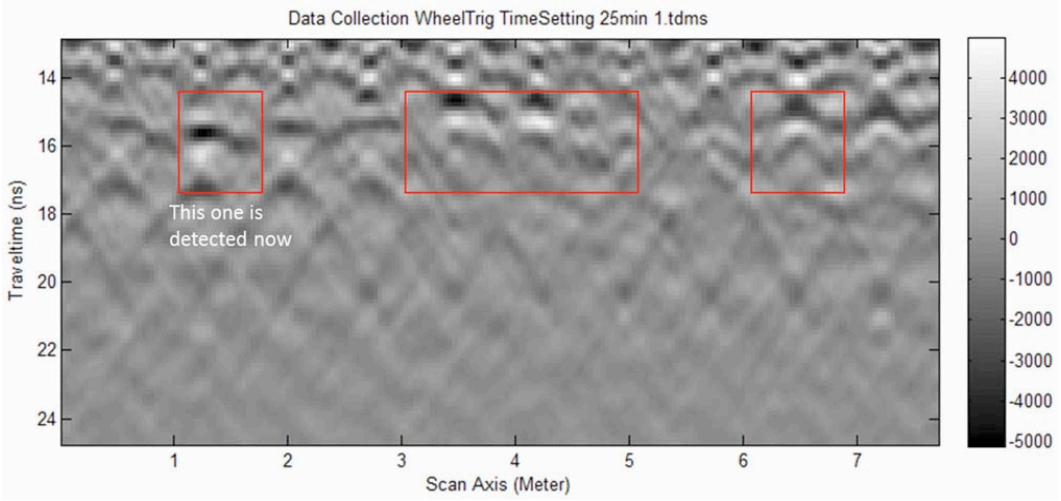

Algorithm 2: Image Migration– Shape Recovery

Stolt's *f-k* Migration: EM wave back projection to the scattering source.

Let $\phi(k, z, f)$ denote the Fourier transform of $\Psi(x, z, t)$ over (x, t)

$$\Psi(x,z,t) = \iint_{-\infty}^{+\infty} \phi(k_x,z,f) e^{2i\pi(k_x x - ft)} \mathrm{d}k_x \mathrm{d}f,$$

Fourier transform to the wave equation yields the Helmholtz equation

$$\frac{\partial^2 \phi}{\partial z^2} + 4\pi^2 \hat{k}_z^2 \phi = 0,$$

the wave number $\widehat{K_z}$ equals

$$\hat{k}_z^2 = \frac{f^2}{\hat{c}^2} - k_x^2.$$

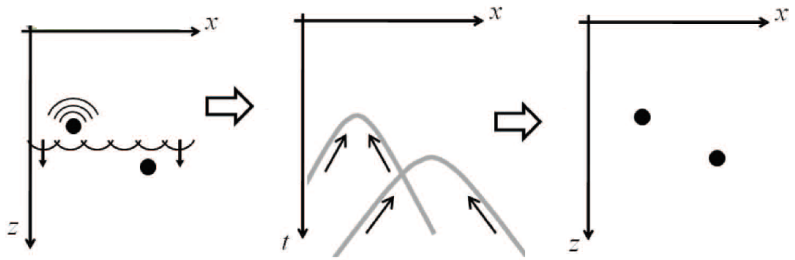

The wave equation can be solved to obtain the migrated wavefield for the buried scatter

$$\Psi(x,z,0) = \iint_{-\infty}^{+\infty} \phi(k_x,0,f) e^{2i\pi(k_x x - \hat{k}_z z)} \mathrm{d}k_x \mathrm{d}f.$$

To employ the Fourier transforms, the variable $\widehat{K_z}$ is changed to

$$f(\hat{k}_z) = \hat{c}\,\mathrm{sign}(\hat{k}_z)\sqrt{k_x^2 + \hat{k}_z^2}.$$

The Stolt's F-K migration solution is

$$\Psi(x,z,0) = \iint_{-\infty}^{+\infty} \frac{\hat{c}\hat{k}_z}{\sqrt{k_x^2 + \hat{k}_z^2}} \phi(k_x,0,f(\hat{k}_z)) e^{2i\pi(k_x x - \hat{k}_z z)} \mathrm{d}k_x \mathrm{d}\hat{k}_z.$$

which is the inverse Fourier transform of

$$\frac{\hat{c}\hat{k}_z}{\sqrt{k_x^2 + \hat{k}_z^2}} \phi(k_x,0,f(\hat{k}_z)).$$

F-K Migration on Real Rebar Inspection Data

F-K migration can help alleviate cross-interference and form focusing dots for each rebar in the image, which facilitates rebar inspections.

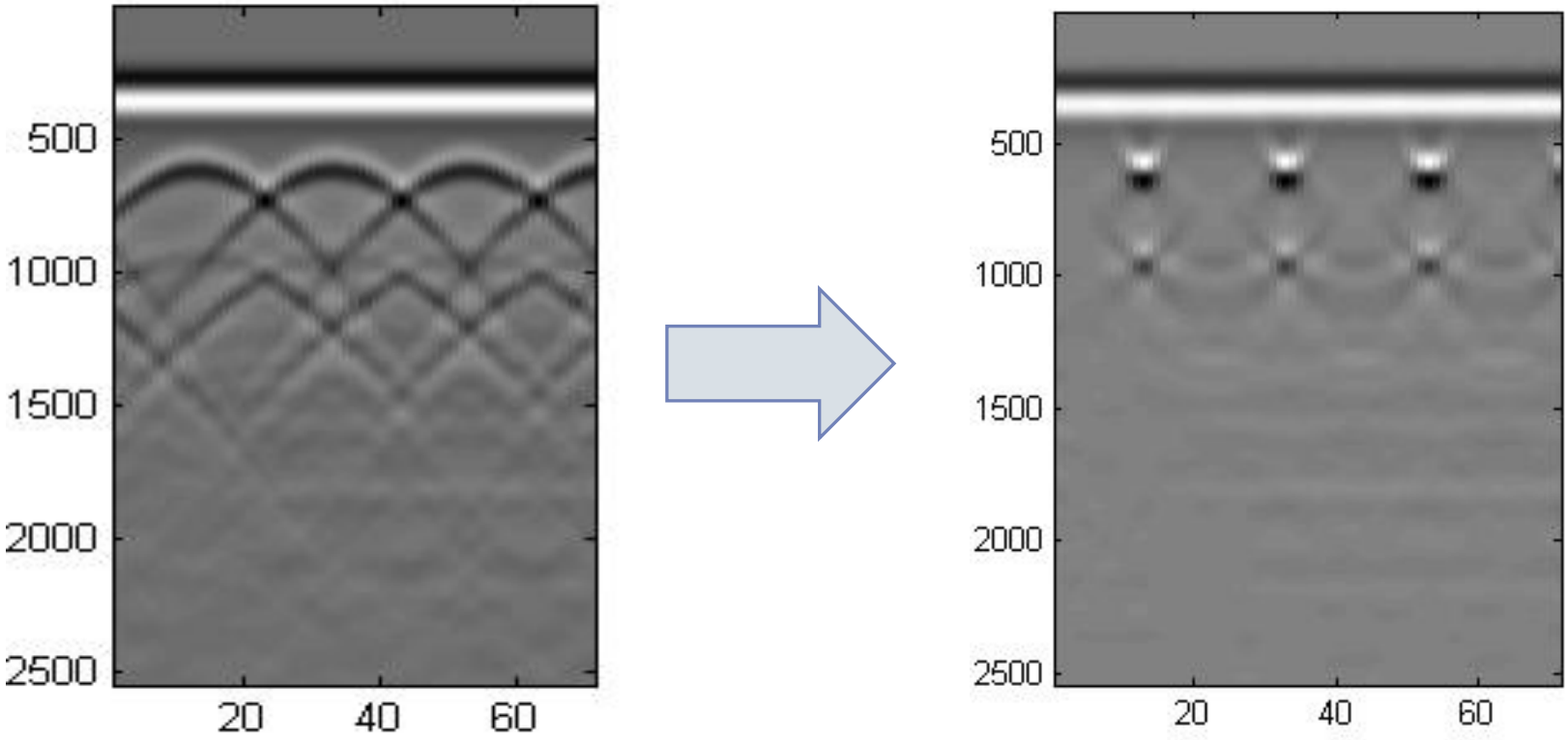

Method 3: Multistatic 3-D Imaging GPR

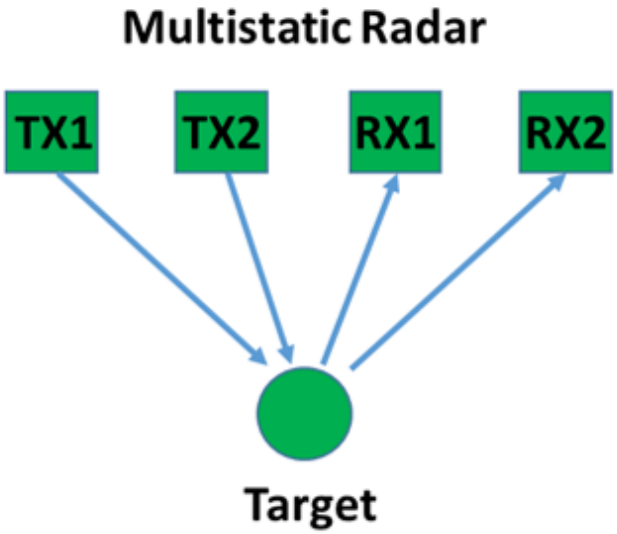

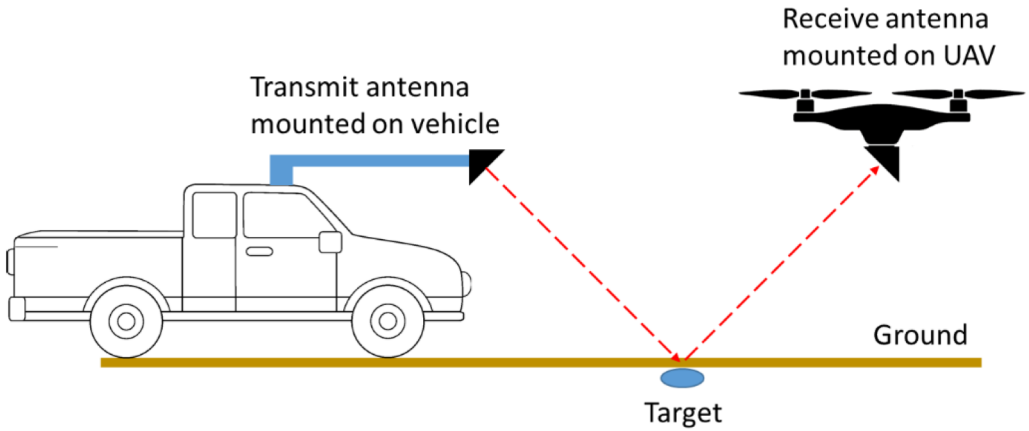

Multistatic Radar

- Spatial diversity offered by the multistatic GPR allows a target being viewed from different aspects – more comprehensive sensing.
- Facilitate fast speed 3D image formation

- Discretize the domain in a finite number of points. Enumerate the position of each GPR antenna pair and enumerate each domain point.
- For the k-system position and the i-domain point, and the p-transmitter and q-receiver in the GPR system, the travel time t_{ik}^{pq} can be stored in an array $T^{pq} = [t_{ik}^{pq}]$.
- The corresponding signal transmitted by antenna pair (*p,q)* at position *k* is $s_{ik}^{pq} = s^{pq}\left(t_{ik}^{pq}\right)$
- Add this signal to $\mathbf{P_i}$, where $\mathbf{P_i}$ is the corresponding space coordinate of the i-domain point $(s_{ik}^{pq}|_{P_i})$
- Repeat for all M system positions, for all (P,Q) pairs in the system, covering all N domain points to form image

$$\mathrm{D} = \sum_{p=1}^{P}\sum_{q=1}^{Q}\sum_{k=1}^{M}\sum_{i=1}^{N} \boldsymbol{A(\theta)} s_{i,k}^{p,q}|_{P_i}$$

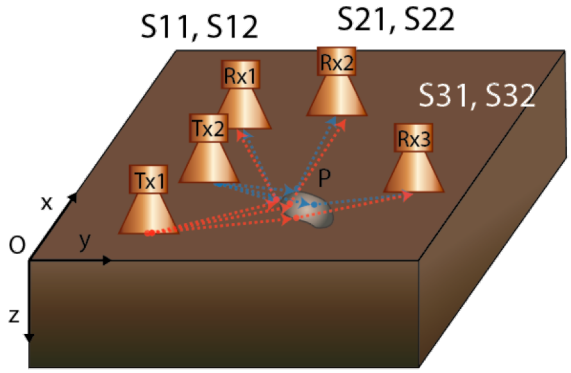

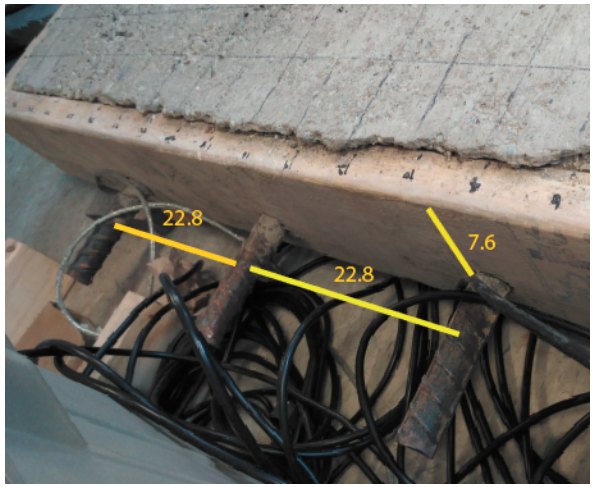

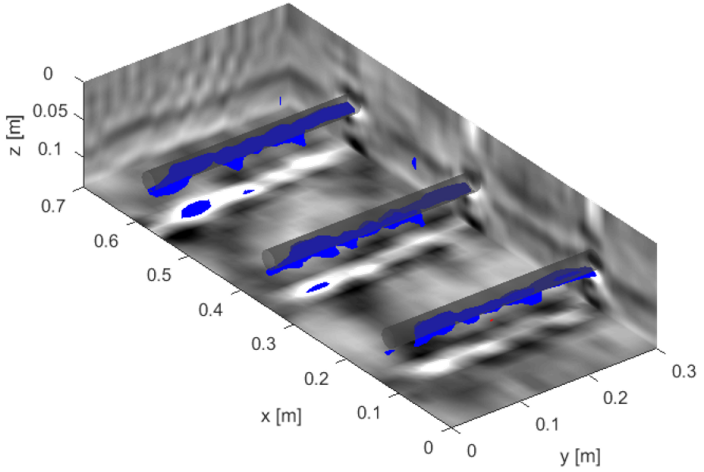

AR based Positioning and Mapping

Precise localization is critically important for:

- Detecting and labeling object positions
- Constructing sensing images;
- Creating accurate maps;

Existing Approaches:

- **GPS:** Limited resolution. Not good for local scale positioning.
  Blocked or and degraded signals in building, tunnels, etc.
- **Wheel encoder:** Assume straight line routing. Not applicable for arbitrary routing; Unable to detect actual route direction and orientations;

Need a better approach

- Sharp accuracy (cm level)
- 3D coordinates
- enable arbitrary survey routing:
- low cost
- reliable

Visual-Inertial Odometry (VIS) for GPR

Integrating computer vision and inertial positioning functions

Perform motion measurement, visual features extraction and data association to achieve precise simultaneous localization and mapping (SLAM).

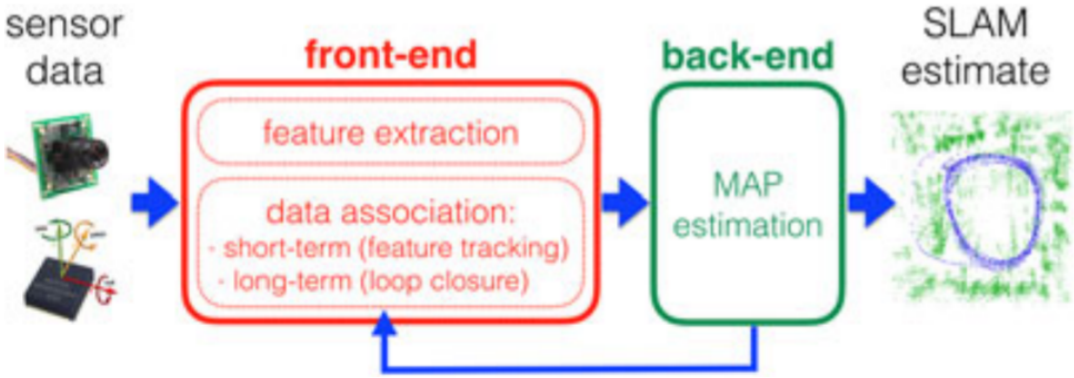

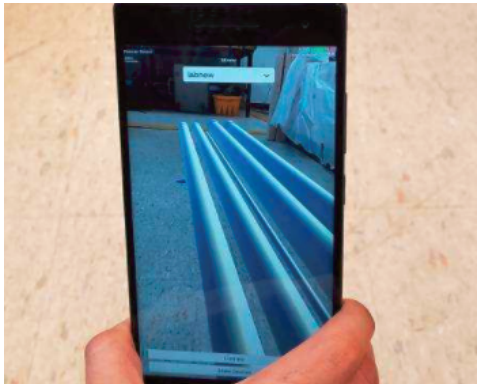

Cadena, C., Carlone, L., Carrillo, H., Latif, Y., Scaramuzza, D., Neira, J., Reid, I. and Leonard, J.J., 2016. Past, present, and future of simultaneous localization and mapping: Toward the robust-perception age. *IEEE Transactions on Robotics*, *32*(6), pp.1309-1332.

IMU Positioning

Inertial Measurement Units (IMUs):

IMU performs **acceleration** $\ddot{x}$ and **angular acceleration** $\ddot{\theta}$ measurements.

Acceleration and angular acceleration are integrated to obtain **velocity** $\dot{x}$ and **angular speed** $\dot{\theta}$.

Velocity and angular speed are integrated to obtain **position** x and θ.

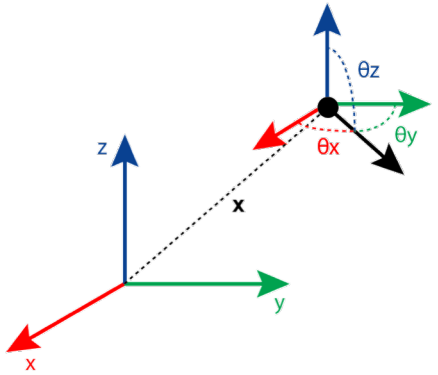

Position

$$x = [x, y, z]$$

Orientation:

$$\theta = [\theta_x, \theta_y, \theta_z]$$

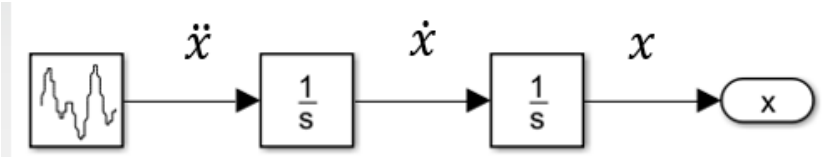

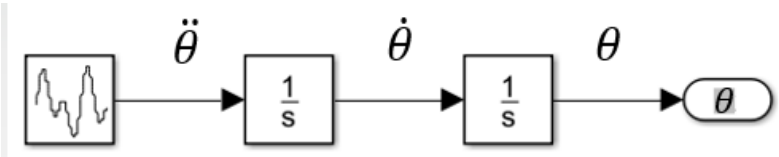

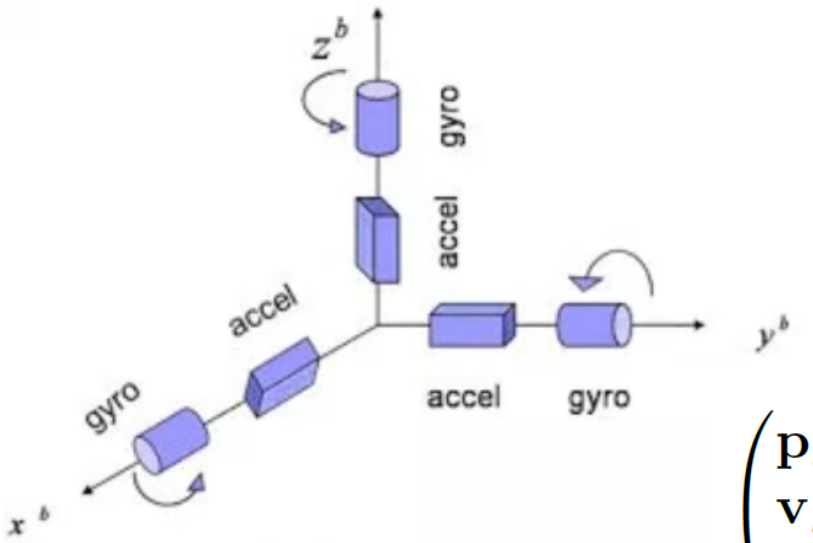

$$\begin{pmatrix} \mathbf{p}_k \\ \mathbf{v}_k \\ \mathbf{q}_k \end{pmatrix} = \begin{pmatrix} \mathbf{p}_{k-1} + \mathbf{v}_{k-1}\Delta t_k \\ \mathbf{v}_{k-1} + [\mathbf{q}_k(\tilde{\mathbf{a}}_k + \boldsymbol{\varepsilon}_k^{\mathrm{a}})\mathbf{q}_k^{\star} - \mathbf{g}]\Delta t_k \\ \boldsymbol{\Omega}[(\tilde{\boldsymbol{\omega}}_k + \boldsymbol{\varepsilon}_k^{\omega})\Delta t_k]\mathbf{q}_{k-1} \end{pmatrix}$$

Visual Augmentation

Estimate position change by comparing feature point locations in subsequent frames.

Appling optimization analysis (i.e. Kalman filter) for IMU and visual data fusion to provide the time-update step and the VIO state estimation.

Creating a map containing the tracked features. The drift is mitigated through a so called loop-closure process.

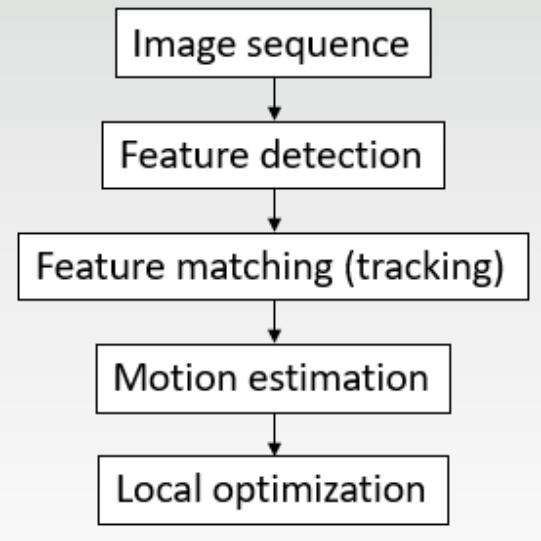

$$\mathbf{x}_k = \mathbf{f}_k(\mathbf{x}_{k-1}, \boldsymbol{\varepsilon}_k)$$
$$\mathbf{y}_k = \mathbf{h}_k(\mathbf{x}_k) + \boldsymbol{\gamma}_k$$

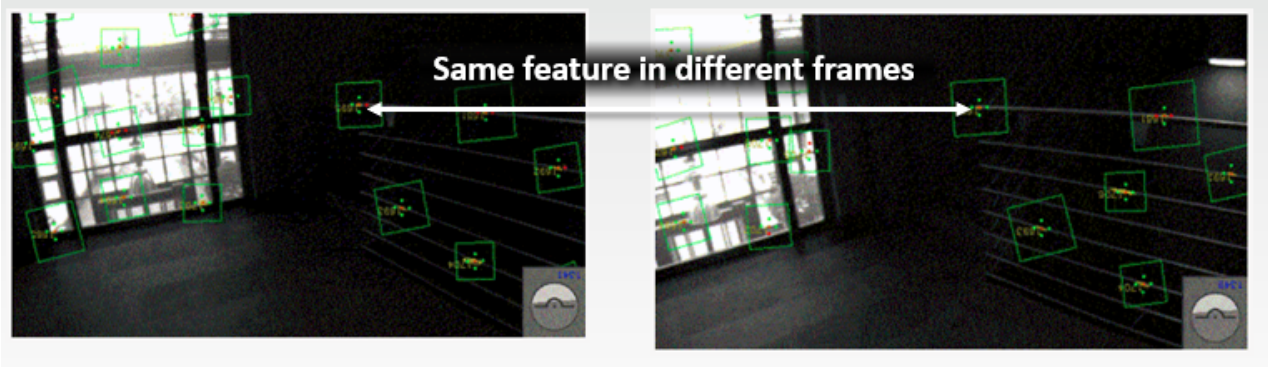

*Images from the ETH Zurich **rovio** project: https://github.com/ethz-asl/maplab

AR Enables GPR Arbitrary Scan Route

The scan does not follow a straight line

- Using Tango device, the circular trajectory can be tracked accurately.
- The underground image feature can be accurately localized and defined by their geographic coordinates through VIO.

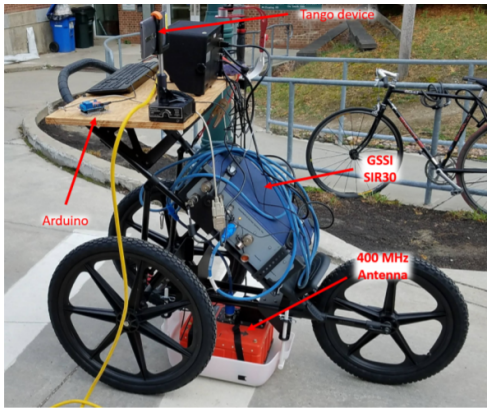

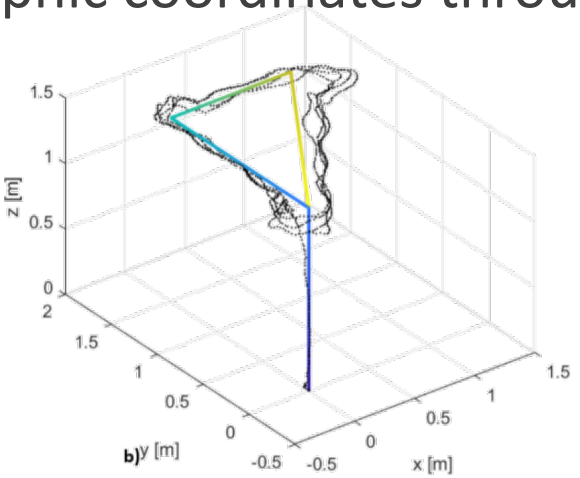

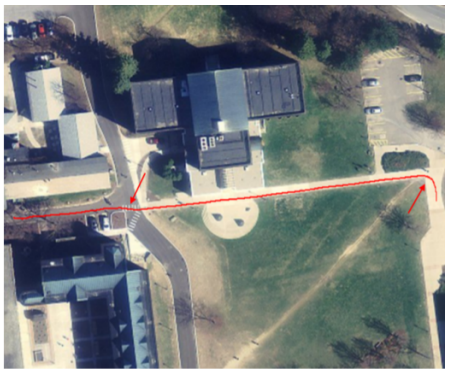

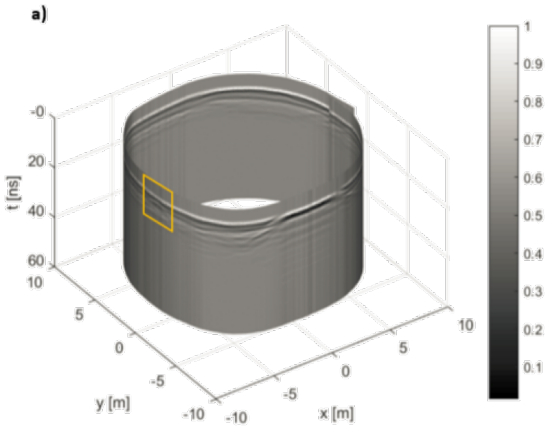

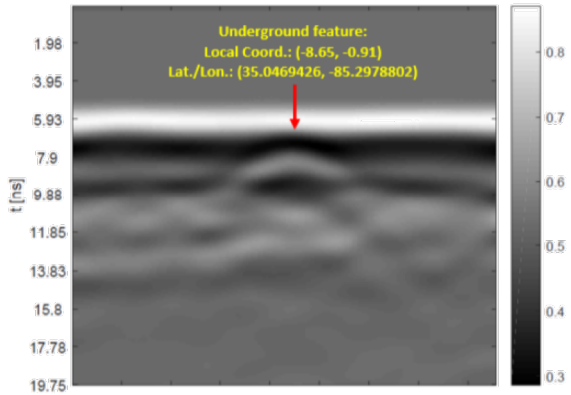

Selected GPR Field Tests

Oct 8, 2015, St. Paul St. , Burlington, VT

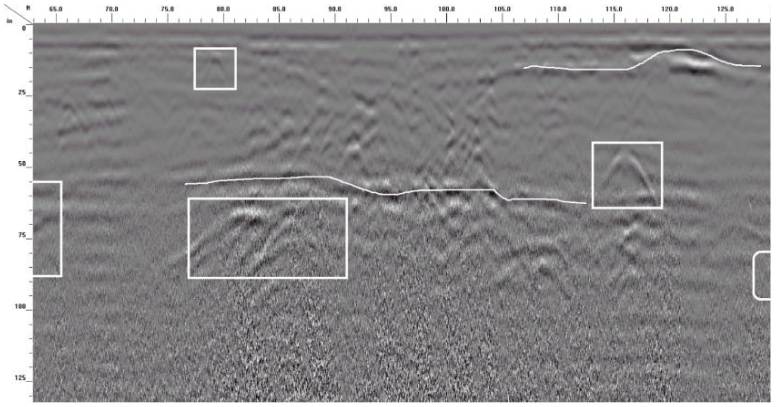

August 2014: MBTA Boston and Metro St. Louis.

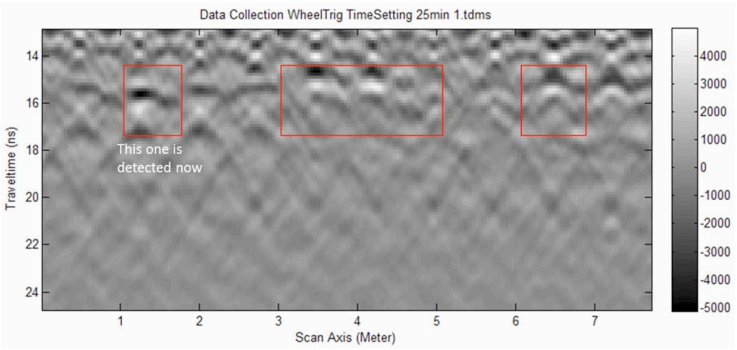

Winooski Railroad Lane Test, May 13 2016.

- Severe fresh water leak
- Rebuild underground infrastructure and paving of street,

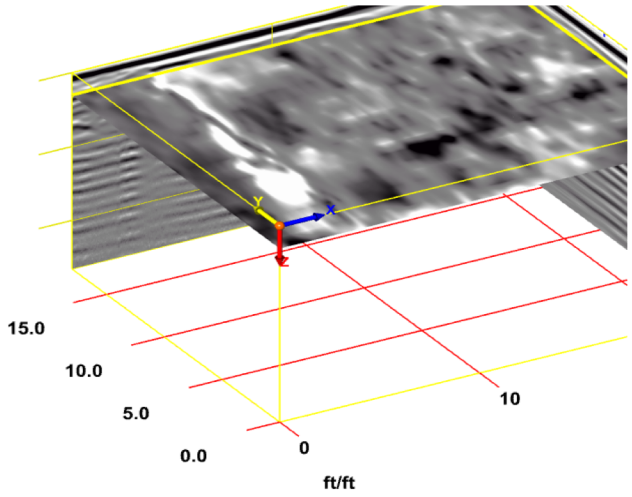

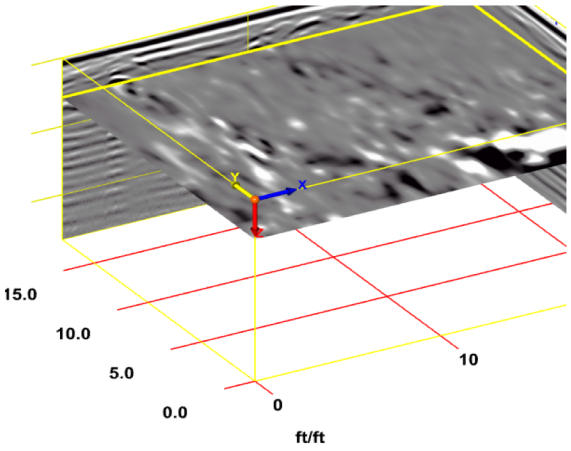

Rotating Magnet Flow Meter System

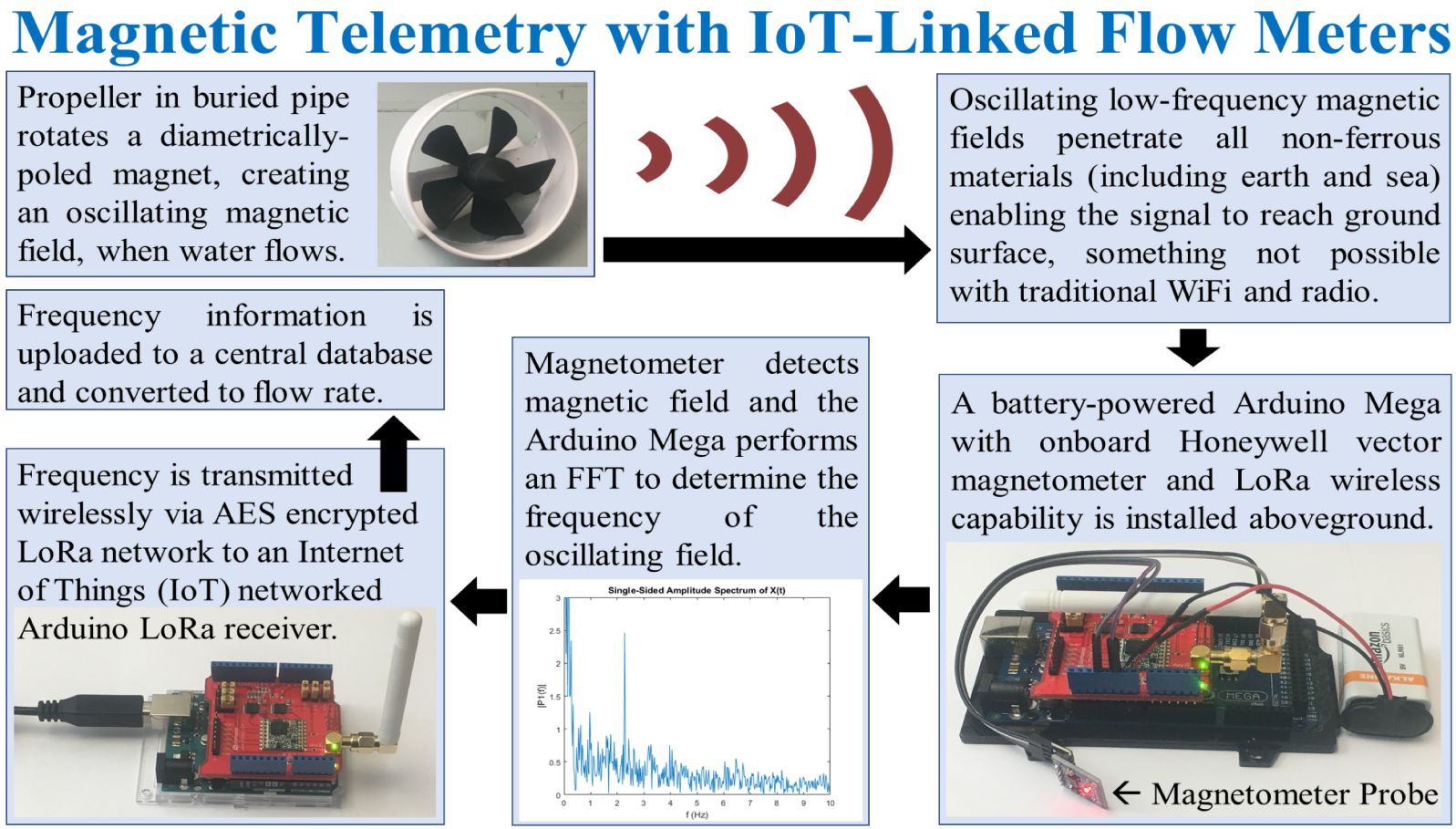

¼ inch diameter magnet cylinder

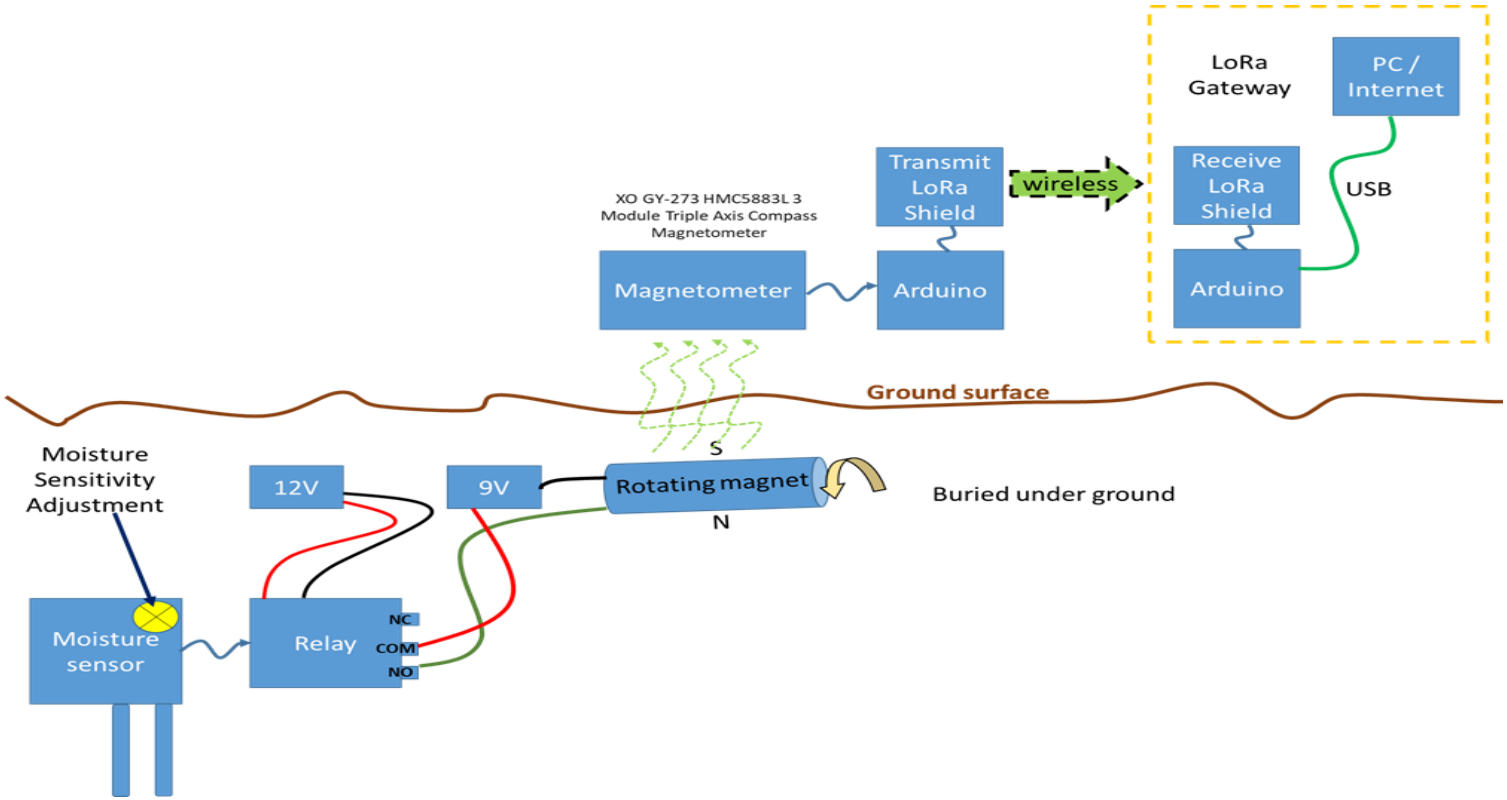
LoRa Gateway
PC / Internet
Transmit LoRa Shield
wireless
Receive LoRa Shield
USB
XO GY-273 HMC5883L 3 Module Triple Axis Compass Magnetometer
Magnetometer
Arduino
Arduino
Ground surface
S
Moisture Sensitivity Adjustment
12V
9V
Rotating magnet
N
Buried under ground
Moisture sensor
Relay
NC
COM
NO

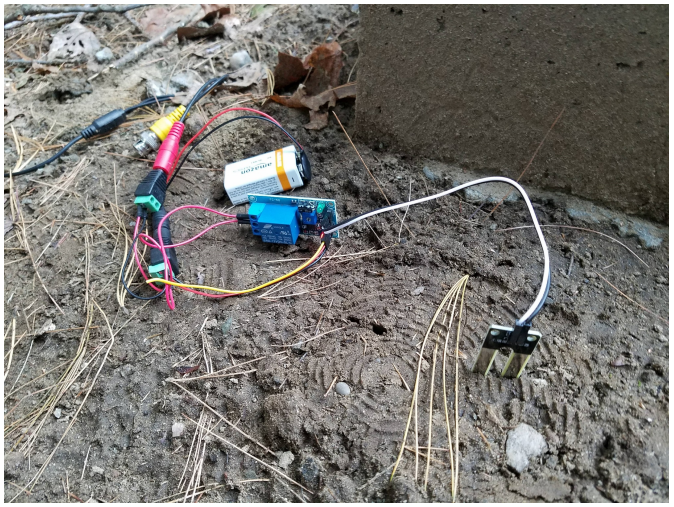

Rotating Magnet Flow Meter Test in Flume

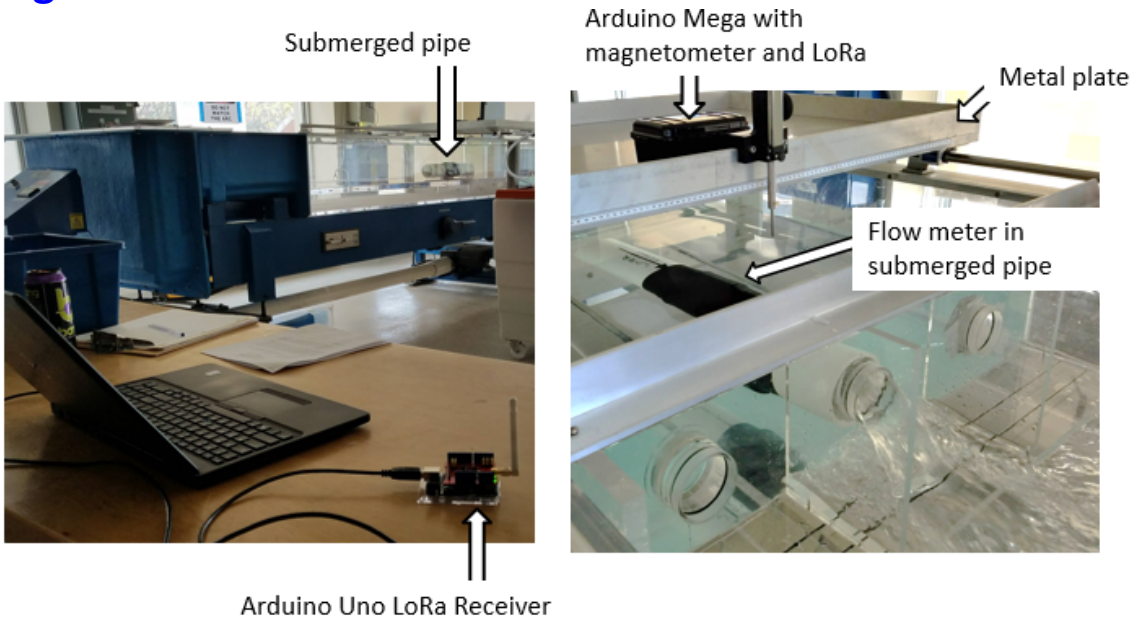

Rotating Magnet Flow Meter in Buried Pipe

12-foot length of 4-inch inner diameter PVC pipe was buried 12-18 inches below ground surface on a hill

	Water flow (Hz)				
	X	Y	Z	Mean	Median
Unburied Pipe	6.59	-	6.57	6.58	6.58
Unburied Pipe—Leak Open	7.60	-	6.19	6.895	6.995
Buried Pipe	3.37 6.24	6.87 6.30	6.84 6.28	5.983	6.29
Buried Pipe—Leak Open	- 7.85	7.25 7.87	7.27 7.86	7.82	7.85

VR for Visualization and Mapping

- HoloLens creates and stores local maps (tied to Wi-Fi connection)
- In a session, virtual objects can be anchored to the local map (e.g. during a survey)
- This enables persistence of holograms between sessions so user can come back at later time and visualize survey data in the correct location

Mapping

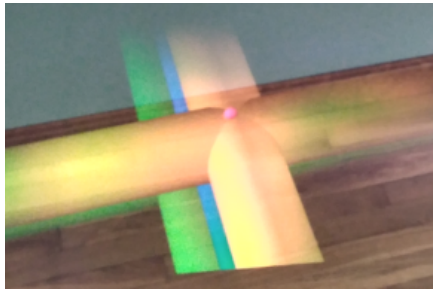

During survey, pipes are positioned in the 3D virtual map matching real position

Visualization

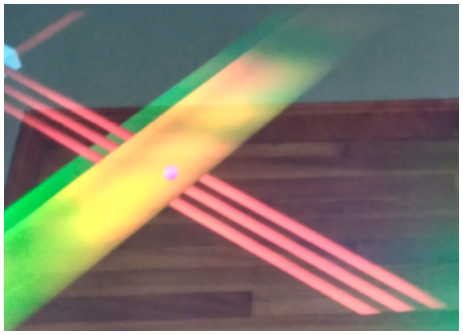

When user starts App, the virtual world won't match the physical world (HoloLens starts at different position)

Visualization + Anchors

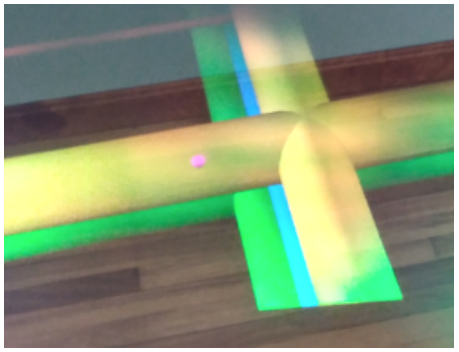

Anchors allow the persistence of holograms. HoloLens matches the stored anchor position to its local map, matching the virtual map to the real world.

Sample Video Clip